POLITECNICO DI TORINO
Repository ISTITUZIONALE

Heat Recovery for a Textile Stenter: CFD Analysis of Air Curtain Benefits

(Article begins on next page)

26 April 2024

Heat Recovery for a Textile Stenter: CFD Analysis of Air Curtain Benefits

Lorenzo Ciappi [1], Daniele Fiaschi [1], Giampaolo Manfrida [1,*], Simone Salvadori [1], Jacek Smolka [2] and Lorenzo Talluri [1]

[1] Department of Industrial Engineering, University of Florence, I50135 Florence, Italy; lorenzo.ciappi@unifi.it (L.C.); daniele.fiaschi@unifi.it (D.F.); simone.salvadori@unifi.it (S.S.); lorenzo.talluri@unifi.it (L.T.)

[2] Institute of Thermal Technology, Silesian University of Technology, 44100 Gliwice, Poland; jacek.smolka@polsl.pl

* Correspondence: giampaolo.manfrida@unifi.it; Tel.: +39-055-2758676

check for
updates

Abstract: Modern textile stenters are designed to reduce the inefficiency of the process and to recover the flow stream, which still contains a relatively high energetic value. In recent years, research has focused on the recovery of the energy content of the low-temperature exhaust flow; nonetheless, another important aspect that may increase the efficiency of the process is the reduction of the ambient air suction. In the present research, an innovative way to improve both machine insulation and energy savings, by using preheated air, was numerically evaluated. The proposed solution utilizes an air stream transverse to the fabric (generally called air curtain), either preheated or not, to create soft gates both at the inlet and at the outlet section of the drying machine. Several valuable advantages can be listed when using this solution: reduction of the dispersion of heat and humid polluted air to the work environment, limitation of air ingestion from outside, and effective heat recovery coupled to a uniform temperature profile around the textile fabric. To analyze the insulation capability of the air curtains in terms of mass and energy transfer, a two-dimensional CFD model of the machine was realized. A test matrix including three possible fabric speeds (20, 40 and 60 m/min), three tilt angles ($-15°$, $0°$ and $15°$), four mass flow rates (0% with no air curtains and 3%, 5% and 7% of the total flow rate through the machine, where the 5% case is equivalent to the flow rate ingested from the ambient) and two temperatures (15 °C and 70 °C) of the plane jets exiting from the air curtains was considered, thus covering a wide range of possible practical applications. The obtained results demonstrate that warm air curtains at both the inlet and outlet are very effective in a fabric speed range up to 40 m/min; at higher fabric speed, entrainment of warm gases from inside the machine at the fabric outlet becomes relevant, and the adoption of a cold air curtain (capable of better insulation) can be recommended in this position.

Keywords: air curtain; textile dryer; stenter; energy saving; computational fluid dynamics

1. Introduction

Over the last years, the world energy scenario has experienced a sharp increase of the energy demand, which has raised attention on several issues, from the exhaustion of resources to the pressing matter of pollutant and greenhouse emissions. This has resulted in the promotion of research into new technologies for energy conversion, as well as in the development of technologies to recover heat that would otherwise be wasted. One of the main sectors involved in this is industrial manufacturing, which accounts for about 38% of the primary energy consumption [1]. To reduce the share of energy consumption, correct management strategies and advanced conversion and utilization technologies

are required [2]. Indeed, the actual fraction of wasted heat in the industrial sector is between 20% and 50% [3].

1.1. Waste Heat Utilization in the Textile Industry

In the most energy-intensive industrial sectors, such as the cement, glass or metallurgical industries, widespread use of energy recovery systems can be found, by which a strong reduction of energy consumption and, consequently, of greenhouse gas emissions may be achieved. An example is provided by the case study of the Kwinana district in Australia, where a significant CO_2 mitigation potential of 245–370 k/year was achieved through energy recovery from flue gas [4].

Another industrial sector with a very high energy recovery potential from its various processes is the textile industry. For instance, only in the USA, the energy consumption amounts to about 87 TWh [1] and its related waste heat share is about 40% [1]. The high value of wasted heat is mainly due to limited information on how to apply energy-efficiency measures [5]. Therefore, there is a compelling interest in introducing solutions to limit the energy wastage. An example is presented in [6], where a summary of the energy saving methods applied to the Taiwanese textile industry is reported. The total savings assessed amounted to 94.6 MWh of electricity (out of which 27.4 MWh was from the process control system), 23.69 m^3 of fuel oil (out of which 17.82 was from the boiler system) and 4.89 t of coal (out of which 4.22 t was from the process control system), just by applying correct management methods. Furthermore, each source of inefficiency was assessed, and a possible reduction solution was also presented. Another work, which focused on the waste heat utilization in the textile industry, was presented in [7]. A quantification of the possible solutions of waste heat recovery from the processes in Bangladesh textile industry, assessing both energy flows and cost, was presented. The analyzed waste heat recovery systems are: (a) heat recovery from generator flue gas, (b) economizers for boilers, (c) waste-heat extraction from dye waste water, (d) steam-condensate recovery, (e) waste-heat recovery from stenter exhaust and (f) blow-down heat recovery.

Further studies on energy optimization management to move towards a sustainable textile industry are introduced in [8] and [9], where a woven manufacturing mill in Bursa (Turkey) was taken as case study. Specifically, in the former, several sustainable systems were assessed, to reduce energy consumption and pollutant emissions. Some of the proposed solutions (reuse of cooling water, renewal of the water softening system) were also implemented, bringing a substantial reduction of water and energy consumption. In the latter, the focus of research was put on a waste heat recovery system. A techno-economic analysis was developed to prove the environmental and economical sustainability of waste heat recovery systems for drying processes in the textile industry. A technical and environmental analysis of another Turkey fabric mill (located in Denizli) was performed in [10]. Particularly, the implementation of 22 Best Available Technologies (BATs), that allow strong reductions of energy consumption and relatively short payback periods, was proposed. In [11], environmental and economical assessments on three different textile factories of the Biyagama Export Processing Zone (Sri Lanka) were performed to demonstrate that environmentally-friendly technology solutions also allow for economic gain.

A significant part of energy consumption in the textile sector is caused by the drying process, which occurs through the utilization of different machines. One of the most used machines for drying fabrics is the stenter machine, which is a large, high-productivity machine that requires a considerable amount of thermal energy to operate correctly. Therefore, several studies were developed on the assessment of the causes of inefficiencies and the possible performance improvement solutions. The exergetic analysis of a real stenter coupled with a boiler and a circulation pump is presented in [12], exploiting the experimental data provided by the factory. The overall assessed exergetic efficiency was found to be 34.4%. Different machine configurations involved a stenter coupled with a conveyor belt dryer [13], proposing a new model for the exergy analysis on convective drying stenters [14] and assessing the influence of several operational parameters on the performance of the machine, such as the drying temperature and the moisture content [15].

Stenter machines are suitable for waste heat recovery system utilization, as the exhaust airflow still has a valuable energy content. This is highlighted in [16] where a drying system with waste-heat recovery is investigated and the energy saving effects as a function of the drying inlet temperature are shown. In [17], the reduction of energy consumption is achieved though the recovery of the waste heat from an indirectly heated stenter, which allows for a strong reduction of coal consumption. The improvement of a low-temperature exhaust indirect heat recovery network for an industrial textile stenter was evaluated in [18], showing the beneficial effects of a targeted redesign of the layout and pipe geometry; the model predictions were positively confirmed by the experimental results. The amount of heat recovered with these improvements was so relevant, that a problem of managing the cold side heat supply is present today. An obvious solution would be to propose combustion air preheating, however this is not simple to implement, because the several gas burners serving the machine are designed for cold air inlet, and the combustion air flow rate is small (in comparison with cold air entering through the fabric inlet/outlet ports) and subject to combustion control adjustment.

1.2. Air Curtains Possible Use in Stenters

Air curtain devices (ACs) were first patented in 1904 [19] as a method to isolate two zones. The first objective of these devices was to "furnish a mean of excluding wind, snow, rain and dust from doorways" as stated in [19]. From its original application, air curtain devices were employed in different fields, such as in safety applications, where the transfer of heat and smoke to a protected ambient can be thus prevented [20]. An experimental investigation of air curtains used as smoke blockage systems, assessing different air curtains velocities, injection angles, slot widths and temperatures and heat rate of the fire, is described in [21]. A recent work applies the air curtain technology to the reduction of dust diffusion during the excavation of tunnels [22], determining the best suited air curtain parameters to achieve a correct dust treatment, reduced energy consumption and cost. Another typical application is the confinement of cold rooms, as it allows the energy consumption reduction of the cooling equipment in applications where the cooled space needs to be open, such as retail stores or commercial display cabinets. This type of application has been deeply assessed, analytically [23], numerically and experimentally [24].

Foster et al. developed a thorough assessment of the optimal jet velocities which are required to achieve high confinement effectiveness [25]. Another parameter, which affects the air curtains performance, is the presence of external lateral flows. A numerical and experimental evaluation was carried out to understand the reduction of effectiveness due to external lateral flows [26]. A specific study on the behavior of air curtains was developed in [27], where a thermography measurement technique was applied. The temperature profile along the central axis of the jet was displayed, confirming that the optimal working conditions correspond to the minimum of the deflection modulus, as stated in [28]. Finally, air curtain applications were studied even in terms of environmental and economic aspects and several analyses were performed to demonstrate the actual attractiveness of such systems compared to the commonly employed ones [29].

Referring to textile machines, sealing more effectively the stenter from cold air ingestion from the fabric inlet/outlet ports is certainly a recommendable practice, allowing one to improve the quality of the work environment and the textile process itself. Application of air curtain technology to stenter machines was addressed in a European project [30]. The provided results claim a 30% energy savings derived from the use of air curtains, mainly due to the reduction of the exhaust flow rate. The novelty of the approach here proposed is to use the air curtain as an efficient heat recovery device: the sealing air is preheated through an indirect heat exchanger (water/air heat exchanger, connected to the waste heat recovery unit for commercial fabric drying machines): the warm air provides a permeable shield, and enters inside the stenter in place of the cold air infiltration, thereby allowing a reduction of the required heat input from the burners. This solution can result in a significant improvement for the field of textile waste heat recovery.

In the present study, air curtains are thus proposed both as a means of shielding a cold inlet flow and as a means for regenerative air preheating, effectively using the heat recovered from the flue gases. The potential savings of the related air curtains are evaluated by the means of dedicated 2D CFD simulations, comparing configurations with or without the air curtains.

2. Description of the Application

2.1. Stenter Geometry

A stenter unit allows wet fabrics, which move across the machine on a horizontal plane at a typical speed between 0.1 and 1 m/s, to be effectively dried through the action of warm air produced by burners and recirculated inside the chamber to obtain a homogenous ambient. A textile stenter has generally a modular structure, where the modules are positioned one after the other in the direction of the moving cloth, as displayed in Figure 1. Each module is composed of an air distribution system, which includes recirculation fans, and specifically designed blowing sections, which ensure the optimal distribution of hot air on the surface of the wet fabric. The number of installed modules depends on the speed of the process, which in turn depends on the type of textile to dry, the wetness of the fabric, the temperature inside of the drying chamber and the ambient conditions. In the present study, a single module of the machine was considered to evaluate the effects of using air curtains to limit the dispersion of heat and effluents to the outside work environment and, at the same time, to reduce the ingestion of ambient air.
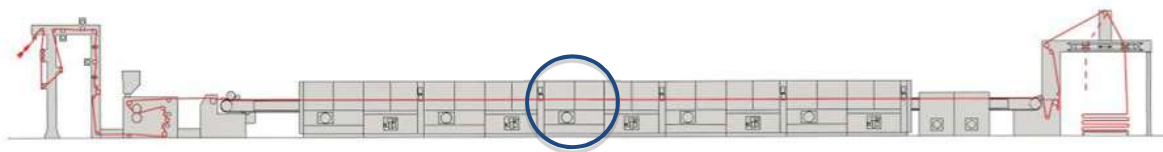

Figure 1. Stenter schematics with highlight of a single module [31].

2.2. Stenter Model

Stenter machines are built in standardized sizes for length and height, while width is dependent on the type of fabric undergoing the drying process. Therefore, if a generalized configuration needs to be considered, a two-dimensional approach must be used, also keeping in mind that the length dimension is the predominant one. For this reason, and to realize a fast prediction model, a simplified 2-D geometry of the machine was selected, by considering a section of the stenter defined by the longitudinal axis and the sagittal axis.

A single module was considered as the effects of air suction on the fabric is particularly relevant in the two zones close to machine inlet and outlet. A 4-stage blowing section is placed within the module, so that the sealing issues should not differ significantly for a single or a multiple-module stenter. The 2-D schematic of a single module of a stenter machine is represented in Figure 2. The recirculated hot air enters the drying chamber through specifically designed arrays of blowing nozzles. The nozzle arrays accelerate and distribute the air flow. They were schematized as porous media in the present study. The hot air passes through the porous media, impacts on the wet fabric and is successively sucked in the recirculation chamber by means of channels positioned between two blowing arrays. The cooled mass flow is recirculated and heated again through mixing with the combustion air coming from the burners and is re-injected through the blowing arrays. Part of the cooled flow rate is expelled from the machine by the means of exhaust fans. This moist stream still has an appreciable energy content: for this reason, in modern stenters the waste heat can be recovered in various forms: it may directly heat up air to be recirculated into the machine or be indirectly recovered to produce hot water.

A feature of the stenter machine is keeping the pressure into the drying chamber below the ambient value. This condition is ensured by the exhaust fans, and it is required to prevent the leakage of combustion gases and effluents from the drying chamber. Indeed, if the combustion gases and

the effluents of the drying process get out of the machine, they may cause serious human health issues, besides environmental pollution. However, as the stenter working chamber operates below the atmospheric pressure, cold air is ingested from both the inlet and outlet slots of the machine, with a relative fraction of the total mass flow between 3% and 7% [12–15]. Ingestion of cold air decreases the machine efficiency and the effectiveness of the drying process. Therefore, to improve the stenter operation, cold airflow from the surrounding environment into the machine should be minimized. From the process point of view, this also improves the quality of the manufactured fabric, as the ingested air may contain dust and other contaminants. The proposed solution to this issue is the use of air curtains at both machine inlet and outlet, as displayed in Figure 3.
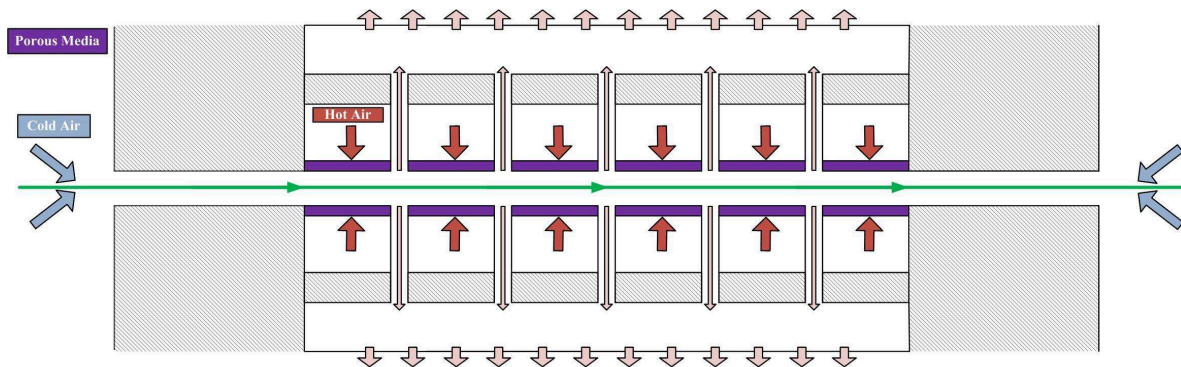

Figure 2. Model scheme without air curtains.

The air curtains configuration shown in Figure 3 takes advantage of the presence, in the modern stenter here investigated, of an indirect heat recovery system for the waste heat: a large fraction of this last is recovered and temporarily stored as warming reservoir (allowing an easy closed-loop distribution through a manifold arrangement). In the present case, the warm water can be used to increase the temperature level of the air flow used to seal the air curtain. The proposed solution should determine the injection of warm sealing air inside the chamber in place of the cold ambient air. For this reason, it is expected that the warm sealing air should determine an increase of the drying efficiency (and consequently a reduction of the required heat input) of the stenter machine. As a high speed of the textile can determine the entrainment of the sealing air outside of the stenter at the outlet section (right), a design alternative with a cold air curtain might be proposed in this position.
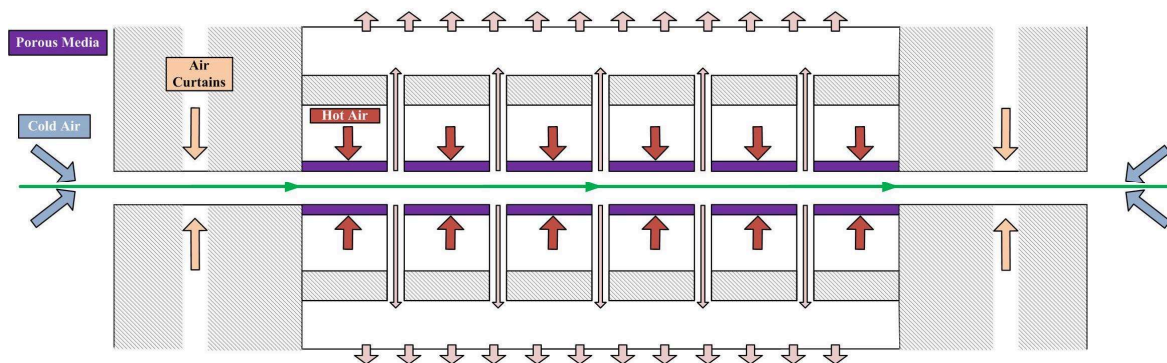

Figure 3. Model scheme with air curtains.

3. Methodology

3.1. Stenter Configurations

The model for the CFD analyses was generated considering the two-dimensional longitudinal section of a single stenter module. Since the machine is vertically symmetrical relative to the textile,

only the upper half of the geometry was created to reduce the use of computational resources and speed up calculations. Three cell zones were defined, as shown in Figure 4 where the main fluid domain, the porous media and the blowing arrays are respectively represented in grey, violet and red. The latter two zones represent the internal recirculation circuit of the machine, while the main fluid domain covers both internal recirculation and the external air. Indeed, a correct fluid domain definition requires that representative portions of the ambient air section both upstream and downstream of the stenter inlet and outlet, as well as the air inside the machine, are considered. The external air regions (dashed light blue line) were sized during preliminary analyses with the aim of modelling the ambient region, which is perturbed by the air flow induced by the machine.

Figure 4. Schematic of the fluid domain used in CFD analyses.

Regarding the geometry, the investigated stenter configurations are four (Figure 5) and vary based on the absence or the presence of the air curtains and on their tilt angle ($-15°$, $0°$ and $+15°$). The tilt angle represents the inclination of the air curtain duct relative to the vertical axis: it is defined positive when the air flow is oriented inward to the machine and negative when the AC is pointing outwards. Indeed, the sign convention for tilt angle, as for all the variables, is that quantities entering the system are considered positive. The aspect ratio of the ACs, defined as the ratio between the width of the AC passage and the gap to be sealed, is 2.5.
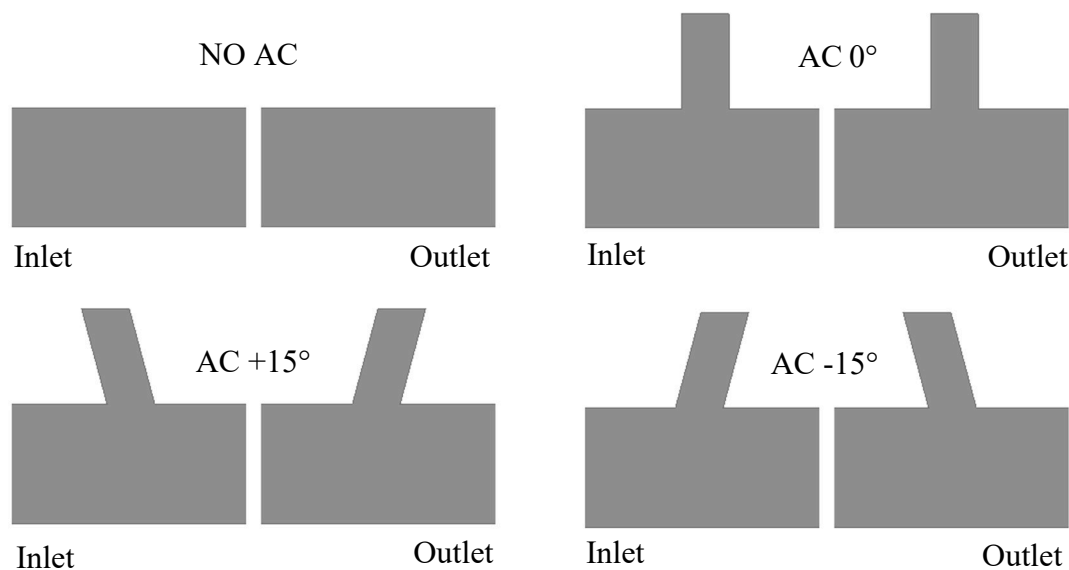

Figure 5. Geometric configurations of the stenter model; (**a**) No air curtain, (**b**) AC tilt angle = $0°$, (**c**) AC tilt angle = $+15°$, (**d**) AC tilt angle = $-15°$.

The geometric configuration without air curtains is the reference case, which is compared with the other configurations to assess the effects of the ACs. The investigated stenter configurations are 60 and differ for fabric velocity, AC temperature and AC mass flow, besides of the geometry in terms of the mentioned AC tilt angle. To cover the most common industrial applications [12], three textile velocities for each of the four geometries presented in Figure 5 and, in addition, two AC flow temperatures to mimic cold and warm air flow and three mass flow rates through air curtains with respect to the ambient air flow for the three geometries with ACs were analyzed. All the considered tilt angles and the operating parameters are listed in Table 1.

Table 1. Parameters determining stenter model configurations investigated with CFD.

AC Tilt Angle (°)	AC Temperature (°C)	AC/Ambient Flow Ratio (%)	Fabric Velocity (m/min)
−15	15	3	0
0		5	20
+15	70	7	40
			60

A porous media assumption was utilized to model the nozzle arrays through which the hot air reaches the main air-drying zone. The geometric parameters of the blowing boxes were selected to model the perforated plates as generally as possible (Table 2).

Table 2. Main geometric parameters of the hot air blowers.

Blower Number (-)	Plate Total Area (m^2)	Plate Open Area (m^2)	Plate Porosity (%)
12	0.7	0.0245	3.5

In Table 3, the coding rules for the several examined configurations are defined. For example, the code AC0CCMV40 identifies a configuration with two air curtains with tilt angle 0°, temperature 15 °C, intermediate flow ratio (5%) and textile speed of 40 m/min while the code NOACV0 states a configuration without air curtains and stationary fabric.

Table 3. Coding scheme based on the parameters from Table 1.

AC Tilt Angle	AC Temperature	AC/Ambient Flow Ratio	Fabric Velocity
−15	C	L	V0
0		M	V20
+15	W	H	V40
			V60

3.2. Numerical Setup

The spatial discretization method utilized in the numerical setup is the finite volume with cell-centered approach. A mapped mesh with quadrilateral elements was generated to discretize the stenter schematic geometry. To assess computational grid independency, a mesh sensitivity analysis was conducted by comparing the results of several diverse meshes with number of elements ranging from 50,000 to 1 million. Since the mesh sensitivity analysis showed a relevant influence of cell dimensions around the fabric, an element refinement in its proximity was done for each grid. The final grid was defined as a compromise between accuracy and computational time: the selected mesh with 260,000 elements fulfils the fixed net mass flux accuracy criterion of 10^{-10} with respect to the specific total mass flux of 0.06185 kg/(s·m). In Figure 6, a close-up of the mapped grid at domain inlet highlighting element structure and distribution is represented.
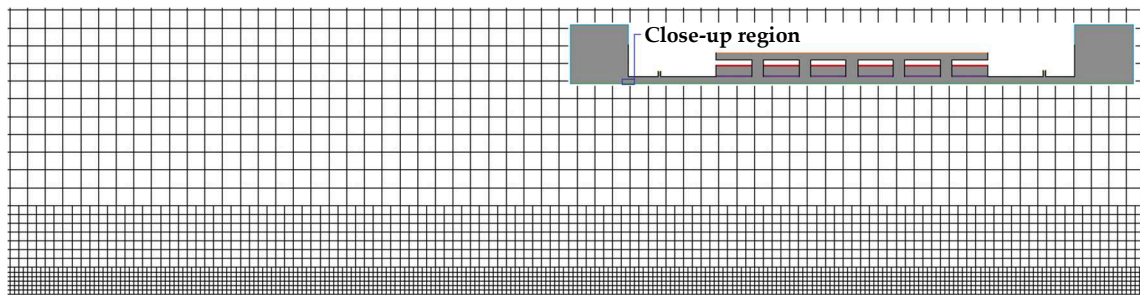
Figure 6. Close-up at fluid domain inlet of the mapped mesh showing element refinement on textile.

The evaluation of the fluid flow through the model was performed with two-dimensional CFD simulations, based on the Reynolds-Averaged Navier-Stokes equations by the ANSYS Fluent 19.1 software [32]. The governing equations are discretized with a cell-centered method with second order scheme for pressure and second order upwind for momentum, turbulent kinetic energy, turbulent dissipation rate, energy and discrete ordinates. To compute the variable gradients, the least-squares cell-based methods were applied.

The turbulence closure was done with the realizable k-ε model standard wall functions for near-wall treatment. Energy exchange was assessed with the discrete ordinate radiation model activated. The equations were implicitly solved by applying the SIMPLE approach [32,33] for coupling pressure and velocity. The boundary conditions of CFD analyses are highlighted with different colors in Figure 7. Air properties were calculated by means of UDFs created for the stenter model.
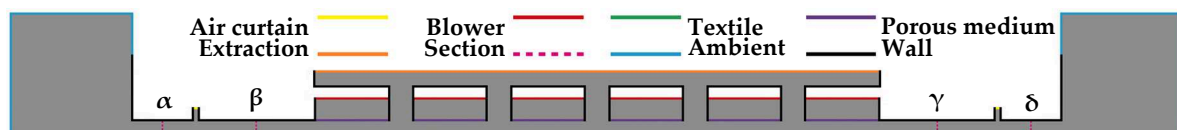

Figure 7. Schematic of the fluid domain with highlighted boundaries and control sections.

Preliminary CFD simulations were carried out on the system without air curtains with steady fabric by imposing the specific mass flow rate at ambient inlet, the specific mass flow rate at heater inlet and the gauge static pressure at extraction outlet (Table 4). As a result, the total pressure at ambient inlet that determines the desired mass flow rate was computed.

Table 4. Main boundary conditions assigned for preliminary CFD analyses.

Boundary	Mass Flow Rate (kg/(s*m))	Total Pressure (Pa)	Total Temperature (K)	Static Pressure (Pa)
Ambient (Inlet)	0.03093	-	288.15	-
Blowers (Inlet)	0.5588	-	473.15	-
Extraction (Outlet)	-	-	-	0

The calculated value of total pressure at inlet was imposed in CFD simulations as the ambient boundary condition; this allows determining and comparing the fluid dynamics of all the 60 investigated configurations, both with and without air curtains (Table 5). The specific mass flow rate of the air curtains was assigned as a fraction of the specific total mass flow rate extracted at the outlet.

Table 5. Main boundary conditions assigned for CFD analyses.

Boundary	Mass Flow Rate (kg/(s·m))	Total Pressure (Pa)	Total Temperature (K)	Static Pressure (Pa)
Ambient (Inlet)		2.71	288.15	
Air curtains (Inlet)	0.01856 (3%)	-	288.15 or 343.15	-
	0.03093 (5%)	-	288.15 or 343.15	-
	0.04330 (7%)	-	288.15 or 343.15	-
Blowers (Inlet)	0.5588	-	473.15	-
Extraction (Outlet)	-	-	-	0

3.3. Performance Indicators

The evaluation of the global performance of the selected air curtains configurations is performed through the definition of a mass sealing effectiveness coefficient and an energy effectiveness coefficient, following a common practice in AC parametrization. The former states the sealing effectiveness of the air curtain in terms of air ingested from the ambient, while the latter states the AC effectiveness of energy recovery in terms of enthalpy. The mass sealing effectiveness coefficient (here reported as ξ_M) is calculated for each configuration equipped with air curtains as the ratio between the mass flow rate passing through a specific control section (CS) and the total mass flow rate exiting the air curtains:

$$\xi_M = \frac{\dot{m}_{CS}}{\dot{m}_{AC}} \tag{1}$$

where $\dot{m}_{CS}$ and $\dot{m}_{AC}$ are the mass flow rates through the control section and the air curtain, respectively. The energy effectiveness coefficient (here reported as ξ_E) is calculated only for the configurations with warm fluid exiting from the ACs at 70 °C as the ratio between the sensible heat flow passing through a specific control section (CS) and the original sensible heat flow rate associated to the air curtain:

$$\xi_E = \frac{\dot{m}_{CS}C_{pCS}(T_{CS} - T_{Amb})}{\dot{m}_{AC}C_{pAC}(T_{AC} - T_{Amb})} = \xi_M \frac{C_{pCS}(T_{CS} - T_{Amb})}{C_{pAC}(T_{AC} - T_{Amb})} \tag{2}$$

where C_{pCS} and C_{pAC} are the specific heat capacities of the air flowing through the control section and the air curtain and T_{CS}, T_{AC} and T_{Amb} are the specific heat capacities of the air flowing through the control section and the air curtain, respectively.

Four control sections were used, two on the left side of the blowing array and two on the right side, positioned at intermediate distance between each ambient opening and the air curtain and between each air curtain and the blowing array. The control sections (α, β, γ, δ from left to right) are shown with dashed lines in Figure 7. For each control section the mass sealing effectiveness coefficient and the energy effectiveness coefficient was calculated.

The target values for ξ_M are the null value for the control section α and δ, that implies perfect sealing, and 0.5 for control sections β and γ, which indicates that the full mass flow rate of the air curtains at machine inlet and outlet respectively is directed inwards. Values of ξ_M higher than these indicate that net flow is entering the stenter, while lower values indicate that net flow is exiting the stenter. By analogy, the targets for ξ_E are zero for control sections α and δ and 0.5 for control sections β and γ to ensure a full exploitation of the air curtain energy input; positive values of ξ_E indicate energy recovery, while negative values represent a waste of energy.

4. Results

4.1. Mass Sealing Effectiveness

The mass sealing effectiveness coefficient (ξ_M) corresponding to the four control sections is presented in function of the AC tilt angle and of the fabric velocity for the three investigated mass flow rates.

The tilt angle configurations are presented in orange ($-15°$, dotted line), green ($0°$, dashed line) and violet ($+15°$, dash-dotted line), with blue pointers for an AC temperature of 15 °C and red pointers for 70°C. In Figure 8 the control section α is considered and it is noticeable that an increase of mass flow rate from 3% to 5% corresponds to a global decrease of ξ_M for each fabric speed; a further increase of AC mass flow rate (up to 7%) reduces furtherly the ξ_M value, but a limited amount of flow leakage across the machine inlet section at the lowest fabric speed appears (negative ξ_M values). The results obtained for the section β (Figure 9) are a consequence of this behavior and indicate that for the highest mass flow rate, with fabric moving at 20 m/min, the air curtain flow is partially directed outside of the stenter, while for all the other configurations it is moved towards into the machine.
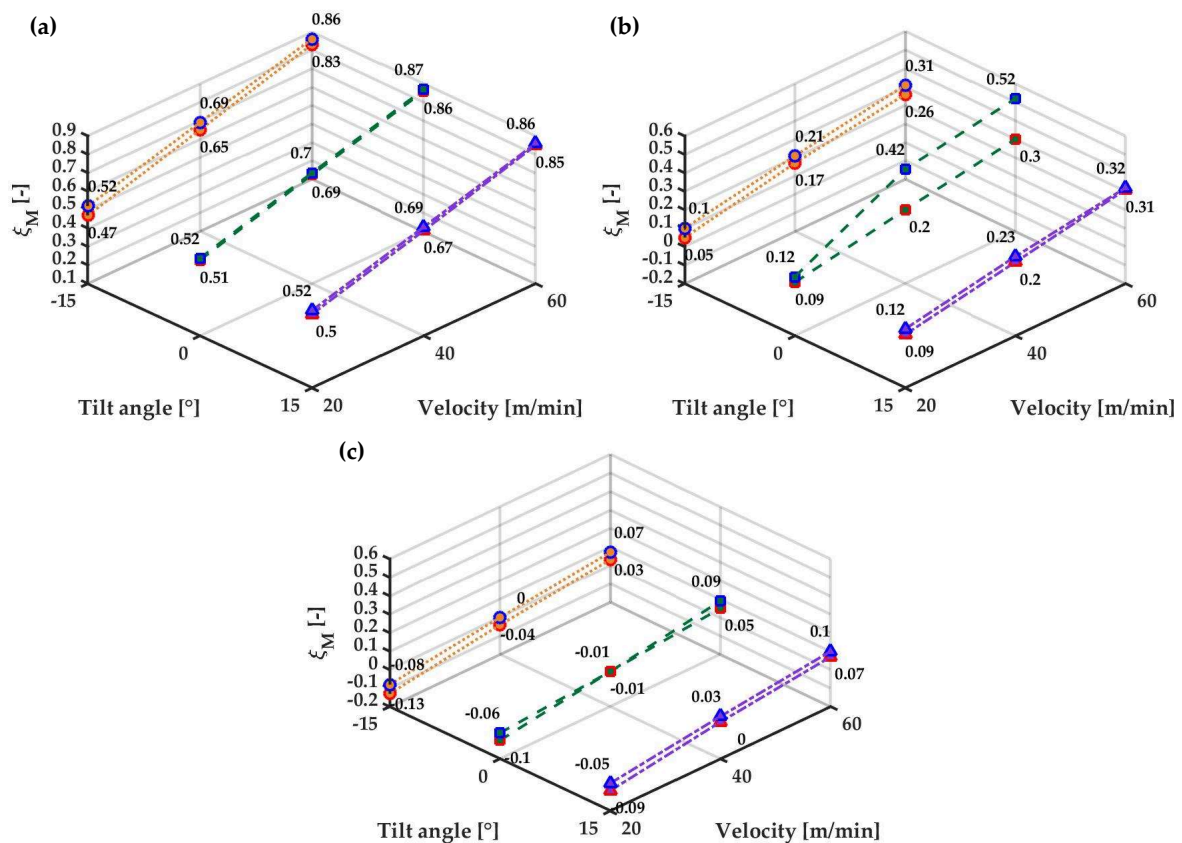

Figure 8. Mass sealing effectiveness coefficient at section α for AC mass flow (**a**) 3%; (**b**) 5%; (**c**) 7%.
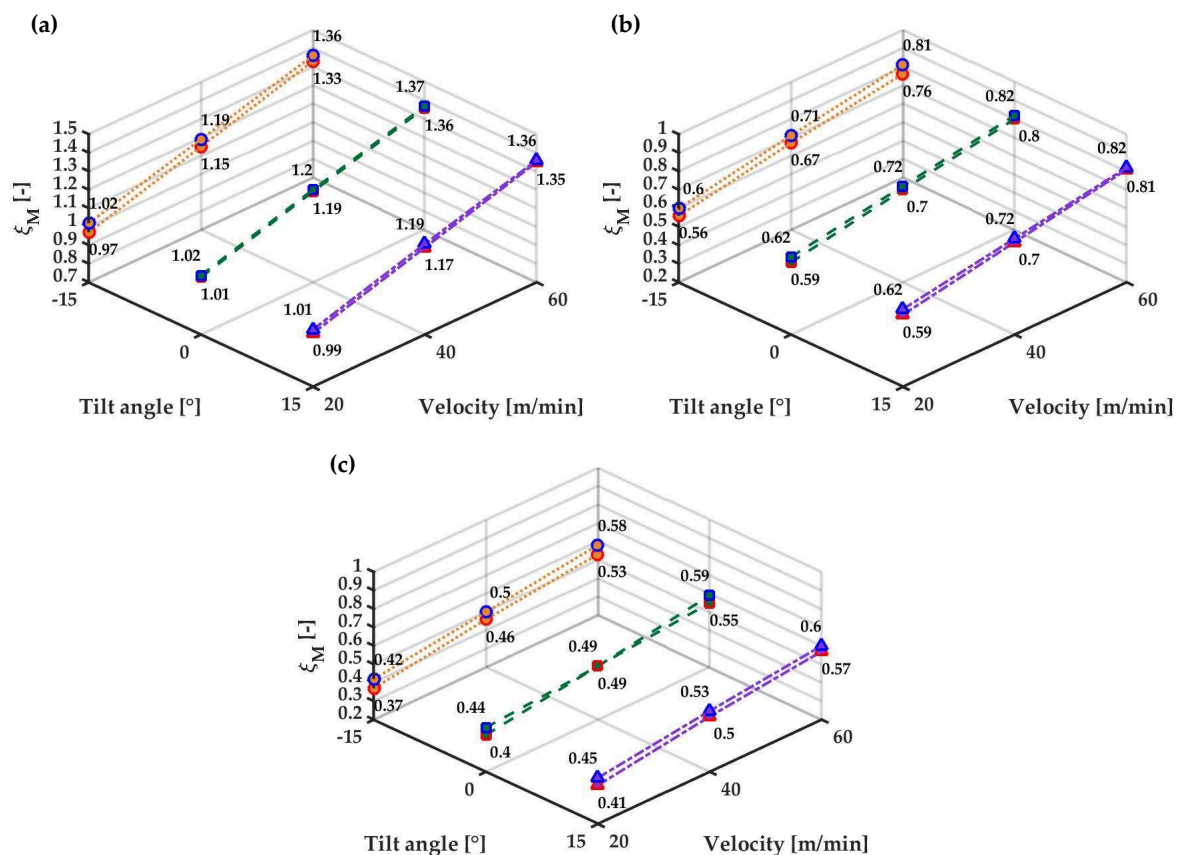
Figure 9. Mass sealing effectiveness coefficient at section β for AC mass flow (**a**) 3%; (**b**) 5%; (**c**) 7%.

In Figure 10, the values of ξ_M on section γ indicate that the sealing efficiency of the air curtains decreases with increasing AC mass flow rate, as the fraction of air entrained by the fabric rises. The mass sealing effectiveness coefficients computed on section δ (Figure 11) indicate that the air curtains can seal the machine outlet only at the lowest fabric speed, when the lowest AC mass flow rate is used; for all the other configurations ξ_M is negative and thus the ACs are unable to provide sealing.

As a general comment on the computational fluid dynamics results, it can be immediately observed that the efficiency and effectiveness of the air curtains mainly depend on the AC temperature and mass flow rate, while the reliance on the AC tilt angle is limited to the impact of the energy effectiveness coefficient for a few specific configurations. Detailed comments on the obtained results follow.

The results achieved for the mass sealing effectiveness coefficients show that the tilt angle of the air curtains has negligible effects on sealing, while the ratio between the mass flow rate of the air curtains and that of the air that would leak towards the ambient in absence of ACs has a key role. Air curtains with low mass flow rate are not useful for sealing the machine openings both at inlet and at outlet and they are only capable of reducing the suction effect. The sealing effect becomes significant when their mass flow rate is equal to the mass flow rate that would be ingested from the surroundings in absence of air curtains. Higher values of mass flow rate would result in a better sealing, but the sealing effectiveness would be worse as indicated by lower values of the related coefficients.
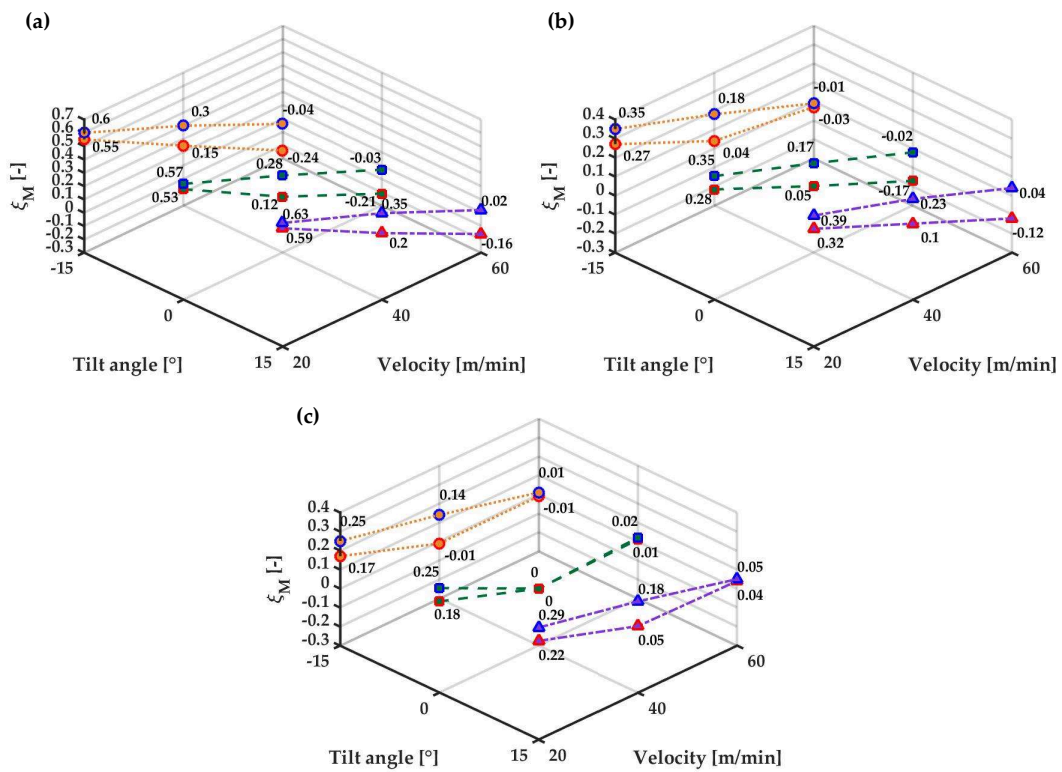
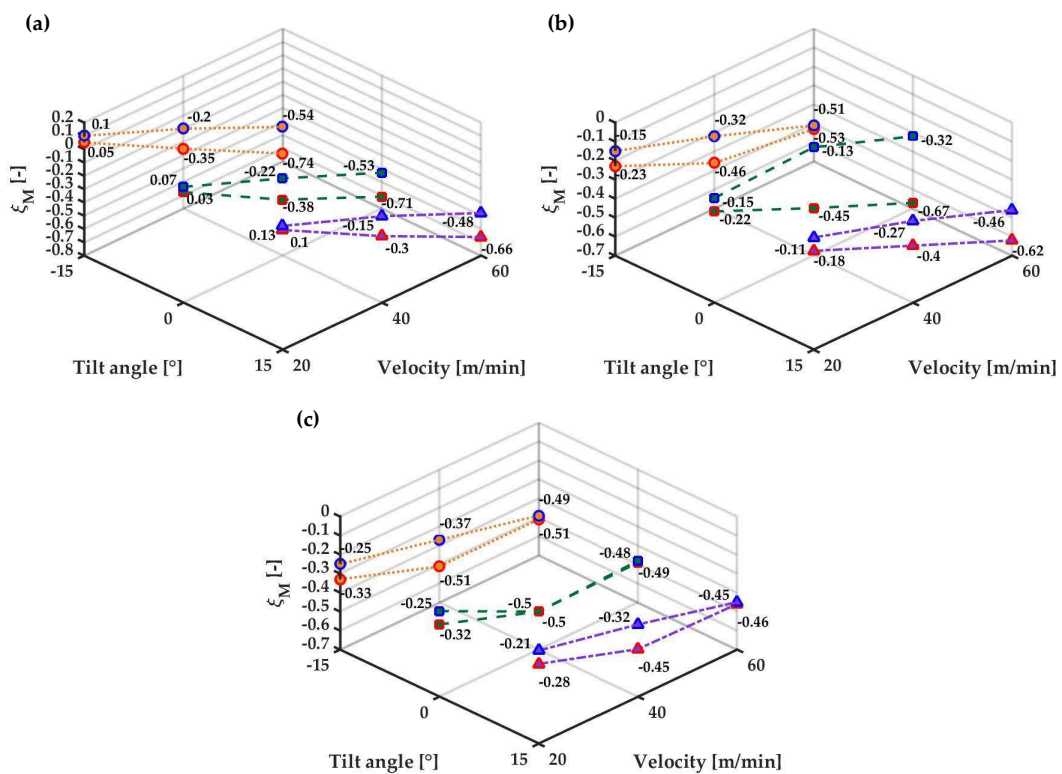**Figure 10.** Mass sealing effectiveness coefficient at section γ for AC mass flow (**a**) 3%; (**b**) 5%; (**c**) 7%.

Figure 11. Mass sealing effectiveness coefficient at section δ for AC mass flow (**a**) 3%; (**b**) 5%; (**c**) 7%.

4.2. Energy Effectiveness

The energy effectiveness coefficient (ξ_E) is represented for the tilt angles $-15°$, $0°$ and $+15°$ with orange (dotted), green (dashed) and violet (dash-dotted) lines respectively only for an AC temperature of 70°C as the purpose is to assess heat recovery potential.

Figure 12 shows that the use of warm air at machine inlet is beneficial for increasing the heat recovery inside of the stenter. In cases (a) and (b) with 3% and 5% of AC mass flow, respectively, the entire mass flow rate of the air curtains is ingested by the machine for each fabric speed, with positive effects on the effectiveness of heat recovery. This means that higher values of this parameter are observed for the increasing values of the fabric velocity. For the case (c) with 7% of AC mass flow rate, a positive value of ξ_E is obtained only at the highest fabric speed, while for lower velocities ξ_E is negative due to partial leakage of the AC mass flow rate.
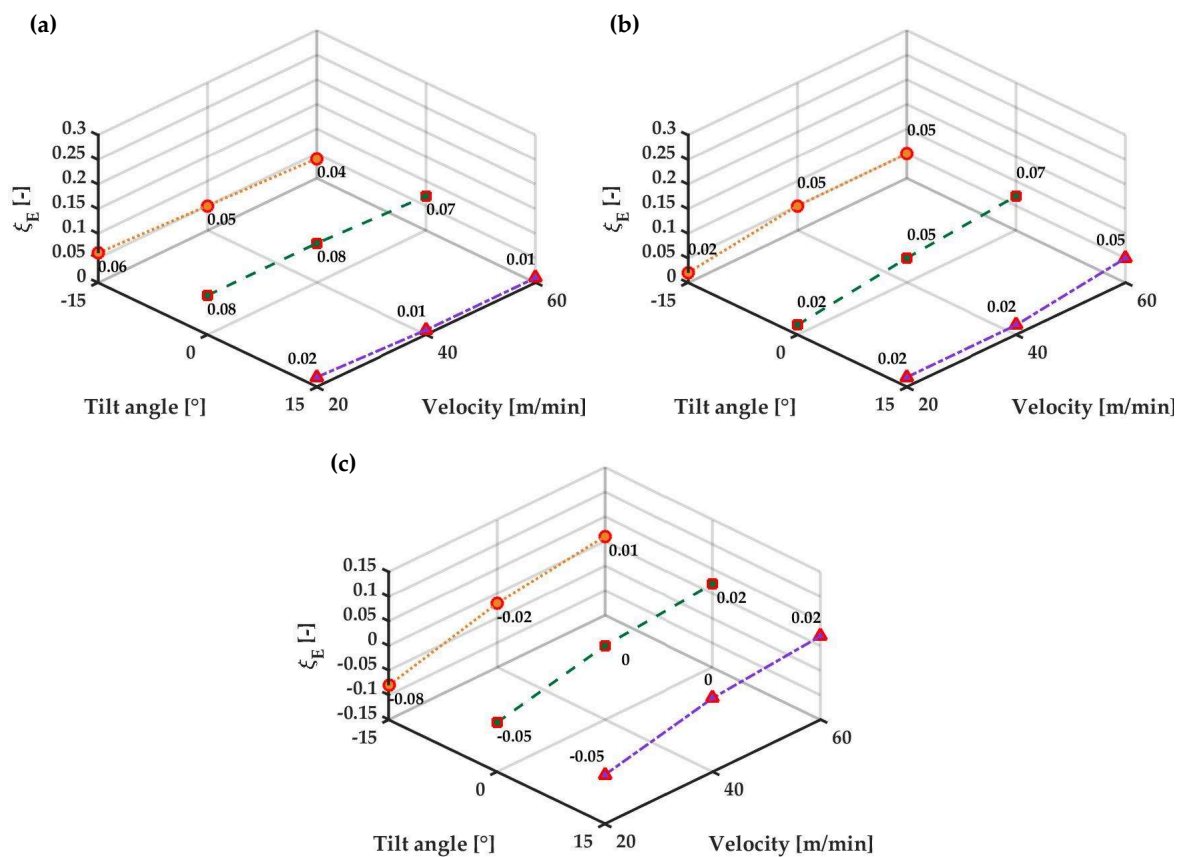

Figure 12. Energy effectiveness coefficient at section α for AC mass flow inlet (**a**) 3%; (**b**) 5%; (**c**) 7%.

In Figure 13, it is noticeable that the tilt angle of the air curtains influences the energy effectiveness. The highest values of the ξ_E are obtained with zero tilt angle air curtains. Nonetheless, that influence is reduced at higher fabric speed and higher AC mass flow rate. At the machine outlet, on section γ (Figure 14), it is evident that the warm air of the air curtains is not correctly recovered. In fact, in most of the cases the ξ_E value is close to 0 or lower when the textile velocity is medium or high, while a positive outcome is visible for low AC flow rates at low fabric velocity. The energy effectiveness coefficients at section δ in Figure 15 confirm this trend with even lower values, thus demonstrating that the heated air is wasted at the machine outlet due to the action of the moving fabric. This clearly indicates that, for the outlet sections, air curtains at ambient temperature, or even the absence of ACs, could be preferred, as the heat recovered would be dispersed in the surrounding environment. The data state that a configuration with air curtains with tilt angles $0°$ or $+15°$ and warm jets (70 °C) and a mass flow rate equal to the mass flow rate that would be ingested from the surroundings without these

devices, provides the best effects. However, at the highest fabric velocity analyzed, a cold air curtain at machine outlet has better parameters. For this reason and to assess the possibility of a reduction of regenerative heat demand, even a mixed configuration with a warm inlet AC (70°C) and a cold outlet AC (15 °C) was analyzed. Since tilted air curtains would imply higher manufacturing complexities than vertical orientation, without significant improvements, only null tilt angles were considered.
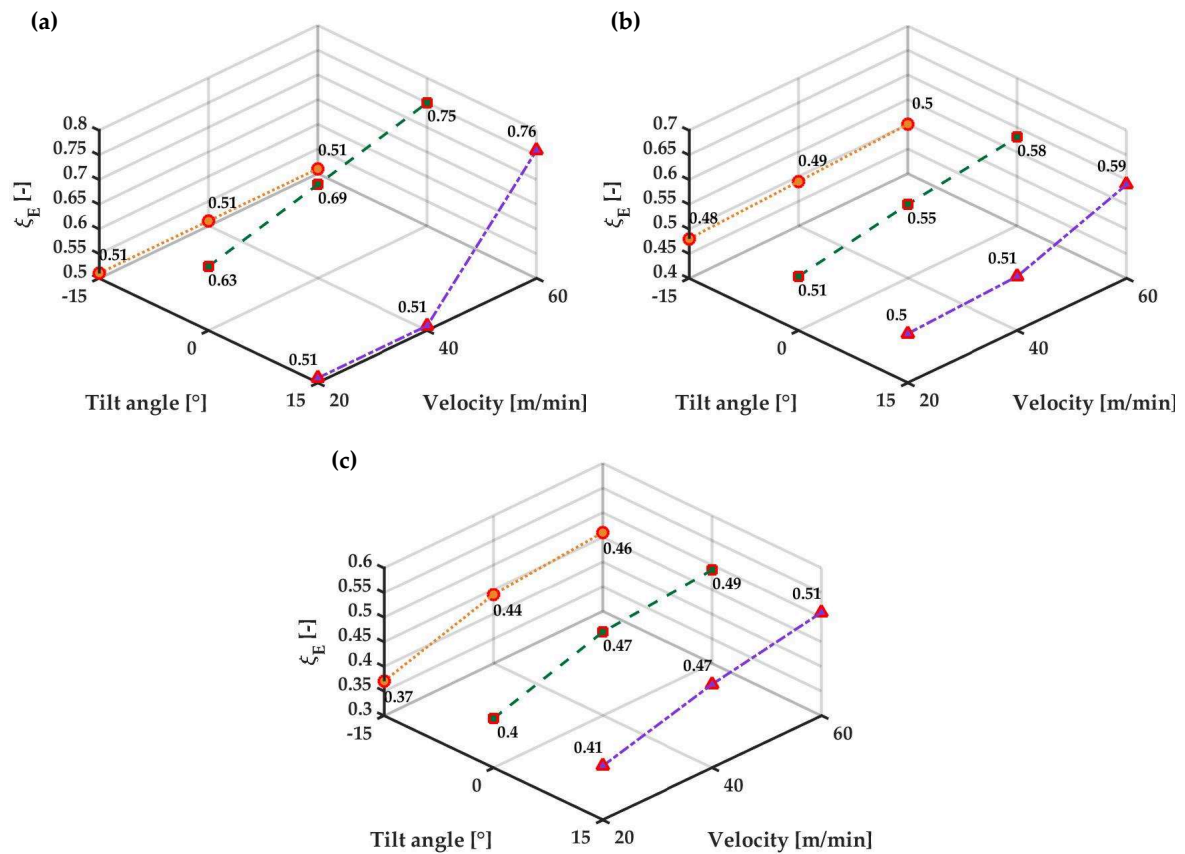

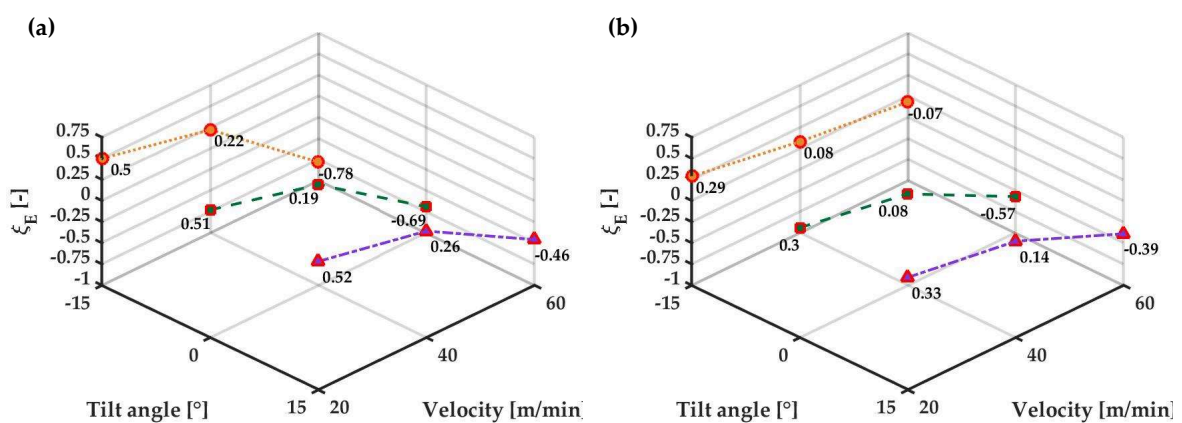**Figure 13.** Energy effectiveness coefficient at section β for AC mass flow inlet (**a**) 3%; (**b**) 5%; (**c**) 7%.

(a)   **(b)**
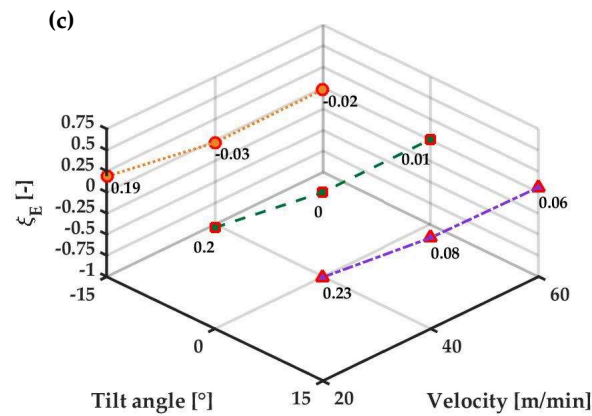

Figure 14. *Cont.*

Figure 14. Energy effectiveness coefficient at section γ for AC mass flow inlet (**a**) 3%; (**b**) 5%; (**c**) 7%.
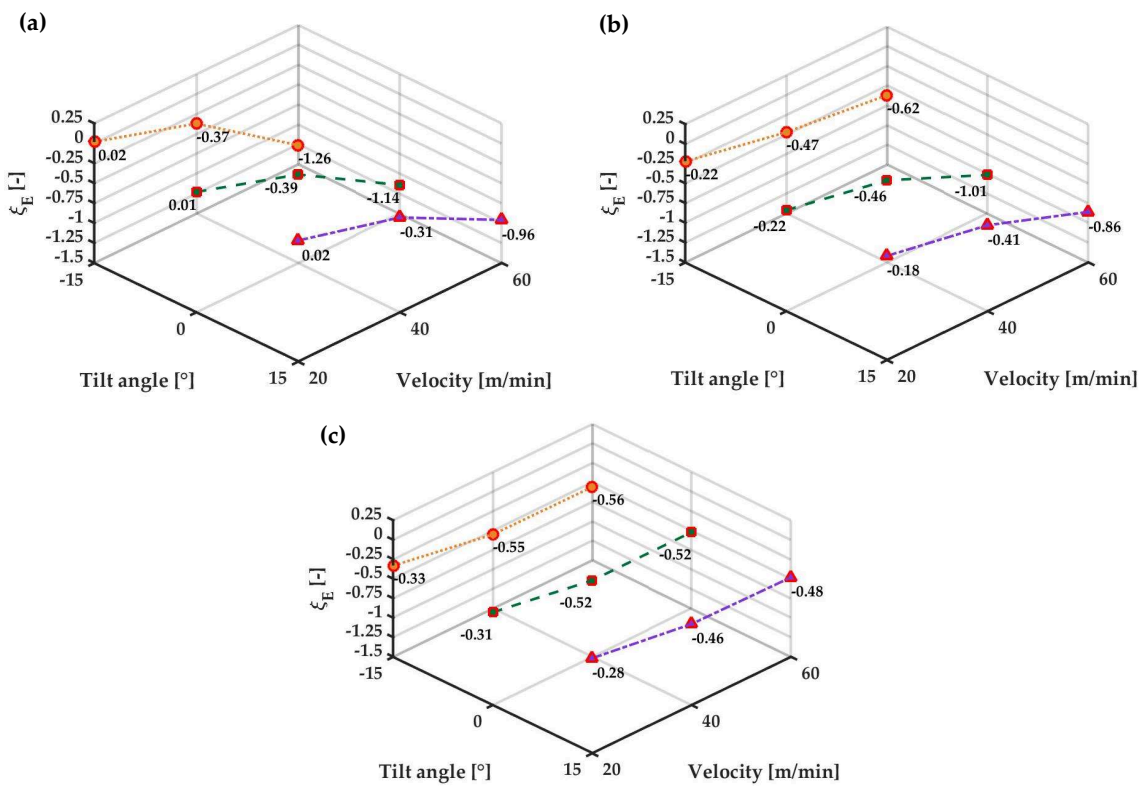

Figure 15. Energy effectiveness coefficient at section δ for AC mass flow inlet (**a**) 3%; (**b**) 5%; (**c**) 7%.

In Tables 6 and 7, the mass sealing effectiveness coefficient and the energy effectiveness coefficient of this configuration are enumerated and compared with those of the similar configuration with both warm air curtains. This implies that a correct selection of AC mass flow rate is fundamental to reach the optimal sealing effect, to prevent the leakage of air both for protection of the workplace environment and to avoid the waste of the warm flow of the air curtains.

Table 6. Mass sealing effectiveness coefficient of the two best air curtain configurations.

Configuration	ζ_E for CS α (-)	ζ_E for CS β (-)	ζ_E for CS γ (-)	ζ_E for CS δ (-)
AC0WWMV20	0.09	0.59	0.28	−0.22
AC0WWMV40	0.20	0.70	0.05	−0.45
AC0WWMV60	0.30	0.80	−0.17	−0.67
AC0WCMV20	0.08	0.57	0.36	−0.14
AC0WCMV40	0.19	0.69	0.18	−0.32
AC0WCMV40	0.28	0.78	0.01	−0.49

Table 7. Energy effectiveness coefficient of the two best air curtain configurations.

| Configuration	ζ_E for CS α (-)	ζ_E for CS β (-)	ζ_E for CS γ (-)	ζ_E for CS δ (-)
AC0WWMV20	0.02	0.51	0.30	−0.22
AC0WWMV40	0.05	0.55	0.08	−0.46
AC0WWMV60	0.07	0.58	−0.57	−1.01
AC0WCMV20	0.02	0.49	-	-
AC0WCMV40	0.04	0.51	-	-
AC0WCMV40	0.05	0.52	-	-

4.3. Temperature Distribution

The air curtains have relevant effects on the temperature distribution inside the stenter at all the investigated fabric speeds. To assess these effects, the adiabatic wall effectiveness coefficient η_{AW} was calculated:

$$\eta_{AW} \triangleq \frac{T - T_{0,Blowers}}{T_{0,AC} - T_{0,Blowers}} \tag{3}$$

where T is the variable temperature and $T_{0,Blowers}$ and $T_{0,AC}$ are the reference temperatures of the blowers (200°C) and of the air curtains (70 °C), respectively. The η_{AW} coefficient is borrowed from the turbomachinery field, where it is used to evaluate the cooling effectiveness of jets in cross-flow [34]. Here it indicates the behavior of air curtains flow and the temperature of air surrounding the fabric, considering adiabatic wall conditions. Null values of η_{AW} mean that the air has the same temperature of the blowers and unitary values state that air has the same temperature of the air curtain; values ranging from 0 and 1 are related to intermediate temperatures, while values greater than 1 denote temperatures lower than that of air curtains (generated by the presence of air ingested from the ambient).

In Figures 16–19, the η_{AW} coefficient distribution of the reference configuration without air curtains (NOAC) is compared with that of the two best configurations identified, with air curtains of zero tilt angle and mass flow rate 5% in both cases and warm jets (AC0WWM) or warm and cold jets (AC0WCM). The color map is limited between 0 and 1 to clearly underline the interaction between the blowers and the air curtains, while the regions where an impact of the ambient flow is foreseen (η_{AW} greater than 1) are in white. The solid line in black represents the η_{AW} distribution on the fabric.
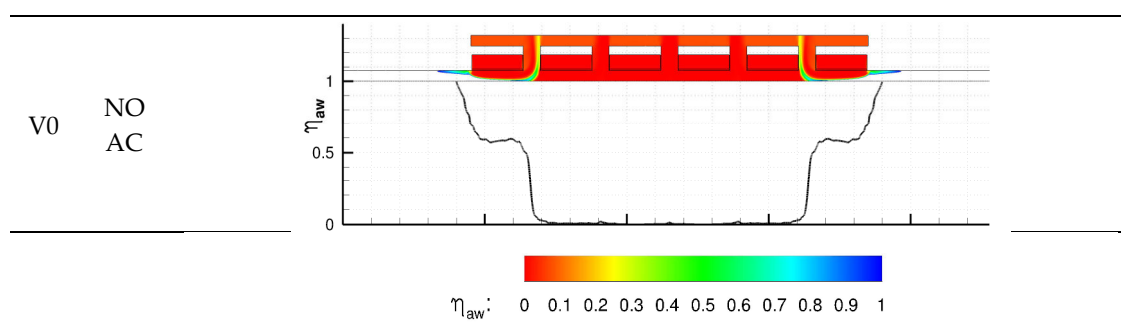
Figure 16. Adiabatic wall effectiveness coefficient distribution for the reference configuration without air curtains and the best configuration with warm air curtains, at 20 m/min fabric speed.

In general, an effective configuration should show a η_{AW} line that reaches the unitary values in correspondence of the AC positions. A η_{AW} line that does not reach the unitary value at the stenter outlet marks a configuration where warm air is wasted outside of the machine. As a general comment on the results, at the stenter inlet, the air curtains allow for a progressive heating of the fabric for each operating condition analyzed; the central part of the cavity is not considerably affected by air flows other than the blower jets; at the stenter outlet the behavior significantly depends on fabric speed.

Figure 16 illustrates the symmetrical distribution of η_{AW} for the reference configuration without air curtains when fabric is steady. In this reference case, the negative influence of cold air entrance is clearly visible, as part of the ambient flow is mixed with the warm air from the blowers. The comparison between the reference case without air curtains at 20 m/min fabric speed and the two best configurations with ACs (Figure 17) shows the beneficial impact of these devices. At stenter inlet, the presence of a warm air curtain determines a negligible variation of the η_{AW} field, but its value on the fabric results to be lower (from 0.55 to 0.45), thus demonstrating that in this case the AC flow substitutes the ambient flow, ensuring a good sealing efficiency.
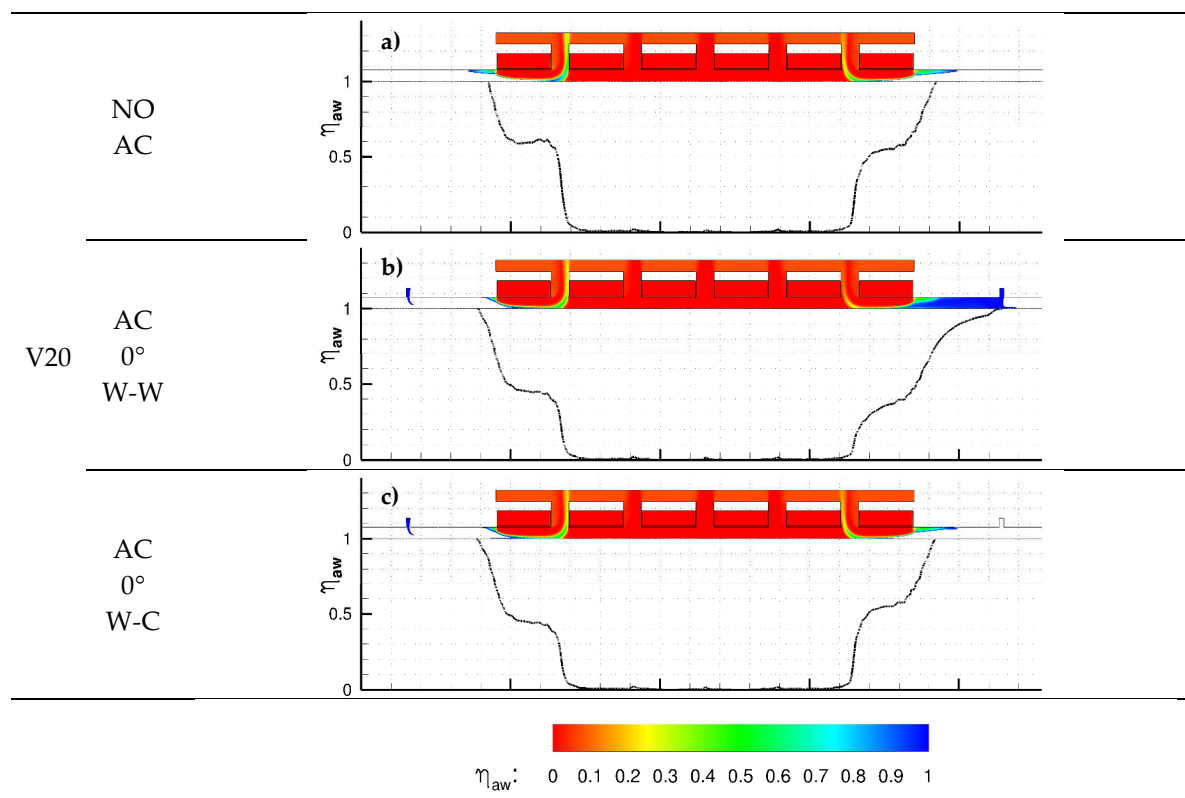

Figure 17. Adiabatic wall effectiveness coefficient distribution for the reference configuration without air curtains and the best configuration with warm air curtains, at 20 m/min fabric speed.

At the stenter outlet, a warm air curtain (b) seems to be preferable to a cold one (c) as the effect of suction caused by the negative pressure difference between the cavity and the environment, overrides the effect of entrainment due to fabric motion. This outcome is supported by the slowest growth of the η_{AW} curve on the fabric, which reaches the unitary value in correspondence of the AC slot and has lower average values, and by the fact that the injected warm air from the AC is not wasted in the ambient.

Figure 18 denotes that the use of air curtains provides some benefits for the fabric, even if its speed rises to 40 m/min. In fact, the distribution of η_{AW} for the warm case shows values around the unit, also after the AC section due to the entrainment of air towards the ambient. This configuration (b) is positive for the drying process because of higher and more uniform temperatures, but the increased

fabric speed makes the sealing action of the AC at the stenter outlet less effective. Instead, the use of cold air from the AC positioned near the stenter outlet (c) generates a η_{AW} map like that obtained without ACs (a), thus suggesting that with this configuration there is no waste of energy and that a certain amount of sealing can be obtained also for high fabric speeds.
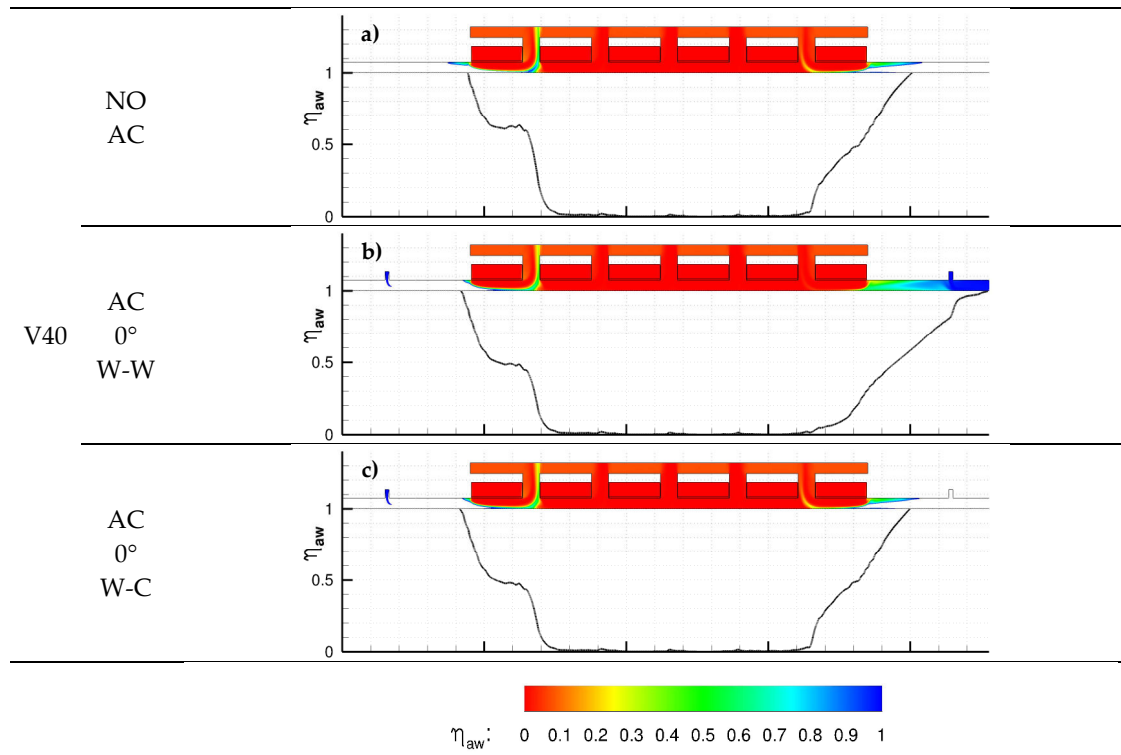

Figure 18. Adiabatic wall effectiveness coefficient distribution for the reference configuration without air curtains and the best configuration with warm air curtains, at 40 m/min fabric speed.

In Figure 19, the worst scenario is represented. In the absence of air curtains (a), it is clearly visible that the fabric is subject to a low η_{AW} value for a great portion of the machine due to a strong entrainment. Although that configuration could be of interest for the fabric warming, a significant amount of hot air exits from the outlet opening and the energy efficiency is greatly reduced. The use of a double-warm air curtain configuration (b) allows for a slight decrease of the η_{AW} values near the stenter outlet (also on the fabric) but the warm flow from the AC is still wasted, as the flow is almost completely entrained towards the exit section. The configuration with the mixed warm-cold air curtains (c) reduces the portion of fabric that is subject to high temperatures, but at the same time is preferable for its higher sealing efficiency (also indicated by the mass sealing effectiveness coefficient closer to zero at control section γ shown in Figure 14) and for its increased thermal efficiency, as there is no waste of energy towards the ambient.

A further analysis of the temperature distribution of the stenter cavity was carried out on a control rectangular area, positioned between the control sections β and γ of Figure 7. The average temperature, the temperature ratio and the mass flow rate ratios were calculated to compare the reference configuration without air curtains and the two best configurations with air curtains (Table 8).

By comparing the average temperatures and the temperature ratios, it is noticeable that the use of air curtains is more effective at low fabric speed and that the configuration with two warm air curtains ensures a higher temperature field as expected. The comparison of the mass flow rate ratios at control section β confirms that both AC configurations have excellent sealing effects. At control section γ it is interesting to note that this parameter quantifies the outcomes of the η_{AW} maps: for a fabric moving

at 20 m/min and 40 m/min a warm air curtain provides better results, while at 60 m/min a cold air curtain is preferable.
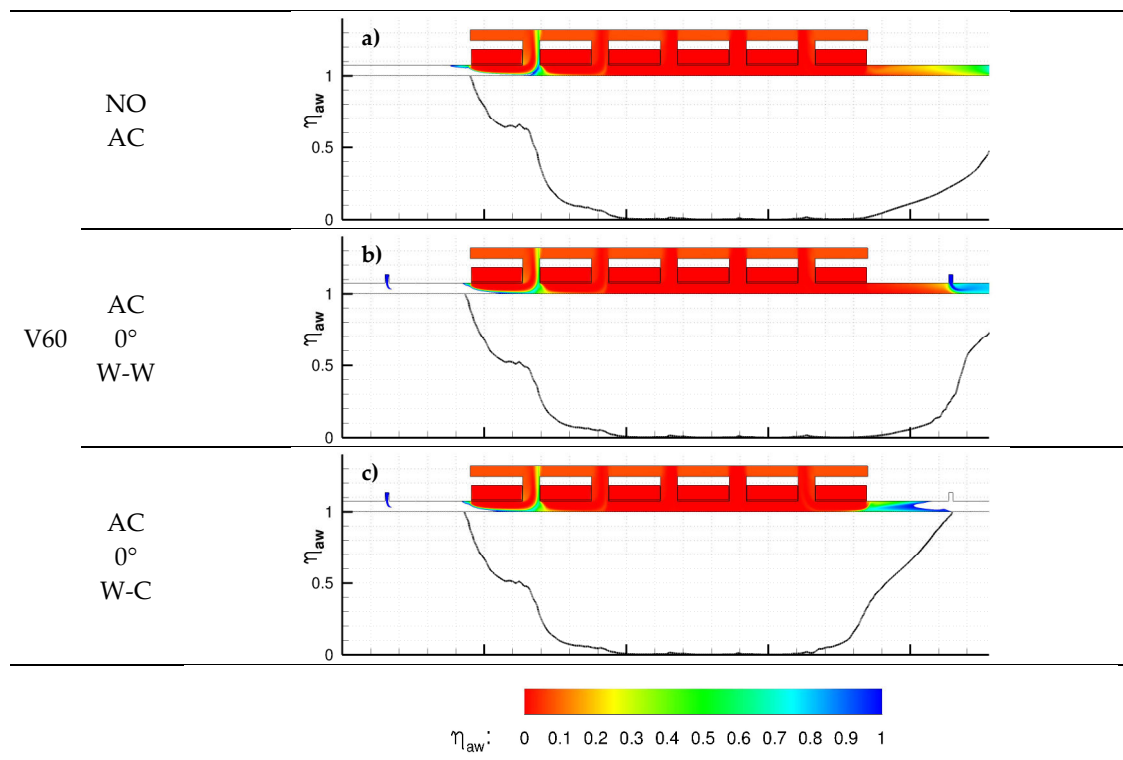

Figure 19. Adiabatic wall effectiveness coefficient distribution for the reference configuration without air curtains and the best configuration with warm air curtains, at 60 m/min fabric speed.

Table 8. Comparison of temperature fields and mass flow rates.

Configuration	Average Temperature (K)	Temperature Ratio (-)	Mass Flow Rate ratio at CS β (-)	Mass Flow Rate Ratio at CS γ (-)
		$\dfrac{\bar{T}_{AC} - T_{AMB}}{\bar{T}_{NOAC} - T_{AMB}}$	$\dfrac{\dot{m}_{withAC}}{\dot{m}_{NOAC}}$	$\dfrac{\dot{m}_{withAC}}{\dot{m}_{NOAC}}$
NOACV20	440.53	-	-	-
NOACV40	442.05	-	-	-
NOACV60	443.67	-	-	-
AC0WWMV20	451.65	11.12	0.96	0.78
AC0WWMV40	452.14	10.09	0.98	0.27
AC0WWMV60	453.51	9.84	0.96	2.03
AC0WCMV20	446.94	6.40	0.94	1.01
AC0WCMV40	448.31	6.26	0.96	1.03
AC0WCMV60	449.17	5.50	0.93	−0.16

5. Conclusions

The novelty of the solution proposed is using the air curtains both as an insulation and as a heat recovery device. The evaluation of the benefits of using air curtains in stenter machines was performed by means of computational fluid dynamics, applying a simplified 2-D model. A wide range of configurations including AC mass flow rate and temperature, fabric velocity as well as different geometrical configurations of the ACs were analyzed. The results state that the installation of the proposed regenerative ACs should allow an appreciable improvement of the machine performance, with reduction of burner heat supply and humid polluted air dispersion to the

surrounding environment, limitation of air ingestion from outside and a proper distribution of air temperature around the fabric.

The key design parameters obtained in this study are the following: the AC configuration with 0° of tilt, mass flow rate 5% and two warm jets (70 °C) provides the best results for fabric speeds of 20 m/min and 40 m/min, while a warm (inlet) and a cold (outlet) AC solution (70 °C and 15 °C) is preferable at 60 m/min. The detailed results can be summarized as follows:

- 60 different configurations were analyzed, determining that the most influencing parameters for air curtains effectiveness are mass flow rate and temperature;
- The tilt angle of the air curtains (−15°, 0° and +15°) has a moderate effect on the machine performance;
- A high AC mass flow rate can result in a negative effect for the stenter, as the recovered heat could be leaked to the environment, as the values of ξ_M and ξ_E are negatively affected;
- The ACs determine an effective reduction of air suction from the environment compared to the reference case without air curtains;
- The use of ACs reduces the energy loss with respect to the reference case and part of the sensible heat used in the ACs is effectively recovered.
- A warm AC is always preferable at the stenter inlet (warm air is ingested by the machine and regeneration is effective)
- At large fabric speeds (above 40 m/min), entrainment of hot gases at the outlet from inside the machine becomes relevant, and a cold AC is recommended at the outlet to improve sealing performance; regeneration can be promoted boosting the flow rate at the inlet warm AC.

Author Contributions: Conceptualization: G.M. and D.F.; Methodology: G.M., L.C., L.T. and J.S.; Software calculations: L.C. and S.S.; Validation: L.C., G.M., S.S. and L.T.; Formal Analysis, Investigation, Resources: All Authors; Data Curation: L.C.; Writing (Original Draft Preparation—Review & Editing): L.C., G.M. and S.S.; Supervision, G.M., D.F., S.S. and J.S.

Conflicts of Interest: The authors declare no conflict of interest.

Nomenclature

Symbols

c_P	Specific heat capacity (J/(kg·K))
$\dot{m}$	Mass flow rate (kg/s)
h	Specific enthalpy (J/kg)

Acronyms

2D	Two-dimensional
AC	Air curtain
AW	Adiabatic wall
CFD	Computational fluid dynamics
CS	Control section

Greek Letters

$\alpha, \beta, \gamma, \delta$	Control sections
ξ_M	Mass sealing effectiveness coefficient
ξ_E	Energy effectiveness coefficient
η_{AW}	Adiabatic wall effectiveness coefficient

Abbreviations

Amb	Ambient

References

1. U.S. Energy Information Administration. International Energy Outlook. 2013. Available online: http://www.eia.gov/outlooks/ieo/pdf/0484(2013).pdf (accessed on 30 November 2018).

2. Zuazua-Ros, A.; Martín Gómez, C.; Ramos, J.C.; Bermejo-Busto, J. Towards cooling systems integration in buildings: Experimental analysis of a heat dissipation panel. *Renew. Sustain. Energy Rev.* **2017**, *72*, 73–82. [CrossRef]

3. Tello, P.; Weerdmeester, R. Spire Roadmap. 2013. Available online: https://www.spire2030.eu/sites/default/files/pressoffice/spire-roadmap.pdf (accessed on 30 November 2018).

4. Beers, D.V.; Biswas, W.K. A regional synergy approach to energy recovery: The case of the Kwinana industrial area, Western Australia. *Energy Convers. Manag.* **2008**, *49*, 3051–3062. [CrossRef]

5. Hasanbeigi, A.; Price, L. A review of energy use and energy efficiency technologies for textile industry. *Renew. Sustain. Energy Rev.* **2012**, *16*, 3648–3665. [CrossRef]

6. Hong, G.B.; Su, T.L.; Lee, J.D.; Hsu, T.C.; Chen, H.W. Energy conservation potential in Taiwanese textile industry. *Energy Policy* **2010**, *38*, 7048–7053. [CrossRef]

7. Rakib, M.I.; Saidur, R.; Mohamad, E.N.; Afifi, A.M. Waste-heat utilization—The sustainable technologies to minimize energy consumption in Bangladesh textile sector. *J. Clean. Prod.* **2017**, *142*, 1867–1876. [CrossRef]

8. Alkaya, E.; Demirer, G.N. Sustainable textile production: A case study from a woven fabric manufacturing mill in Turkey. *J. Clean. Prod.* **2014**, *65*, 595–603. [CrossRef]

9. Pulat, E.; Etemoglu, A.B.; Can, M. Waste-heat recovery potential in Turkish textile industry: Case study for city of Bursa. *Renew. Sustain. Energy Rev.* **2009**, *13*, 663–672. [CrossRef]

10. Ozturk, E.; Koseoglu, H.; Karaboyaci, M.; Yigit, N.O.; Yetis, U.; Kitis, M. Sustainable textile production: Cleaner production assessment/eco-efficiency analysis study in a textile mill. *J. Clean. Prod.* **2016**, *138*, 248–263. [CrossRef]

11. Shiwanthi, S.; Lokupitiya, E.; Peiri, S. Evaluation of the environmental and economic performances of three selected textile factories in Biyagama Export Processing Zone Sri Lanka. *Environ. Dev.* **2018**, *27*, 70–82. [CrossRef]

12. Cay, A.; Tarakcioglu, I.; Hepbasli, A. Exergetic performance assessment of a stenter system in a textile finishing mill. *Int. J. Energy Res.* **2007**, *31*, 1251–1265. [CrossRef]

13. Cay, A.; Tarakcioglu, I.; Hepbasli, A. A study on the exergetic analysis of continuous textile dryer. *Int. J. Exergy* **2009**, *6*, 422–439. [CrossRef]

14. Cay, A.; Tarakcioglu, I.; Hepbasli, A. Exergetic analysis of textile convective drying with stenters by subsystem models: Part 1—Exergetic modelling and evaluation. *Dry. Technol.* **2010**, *28*, 1359–1367. [CrossRef]

15. Cay, A.; Tarakcioglu, I.; Hepbasli, A. Exergetic analysis of textile convective drying with stenters by subsystem models: Part 2—Parametric study on exergy analysis. *Dry. Technol.* **2010**, *28*, 1368–1376. [CrossRef]

16. Oğulata, R.T. Utilization of waste-heat recovery in textile drying. *Appl. Energy* **2014**, *79*, 41–49. [CrossRef]

17. Sekkeli, M.; Keçecioglu, O.F. Scada based an energy saving approach to operation of stenter machine in a textile plant using waste-heat recovery system. *J. Text. Appar./Tekstil ve Konfeksiyon* **2012**, *22*, 248–257.

18. Fiaschi, D.; Manfrida, G.; Russo, L.; Talluri, L. Improvement of waste heat recuperation on an industrial textile dryer: Redesign of heat exchangers network and components. *Energy Convers. Manag.* **2017**, *150*, 924–940. [CrossRef]

19. Van Kennel, T. Means for Excluding Drafts from Open Doorways. U.S. Patent 774,730, 8 November 1904.

20. Krajewki, G.; Wegrzynski, W. Air curtain as a barrier for smoke in case of fire: Numerical modelling. *Bull. Pol. Acad. Sci. Tech. Sci.* **2015**, *63*, 145–153.

21. Yu, L.X.; Liu, F.; Beji, T.; Weng, M.C.; Merci, B. Experimental study of the effectiveness of air curtains of variable width and injection angle to block fire-induced smoke in a tunnel configuration. *Int. J. Therm. Sci.* **2018**, *134*, 13–26. [CrossRef]

22. Liu, Q.; Nie, W.; Hua, Y.; Peng, H.; Liu, C.; Wei, C. Research on tunnel ventilation systems: Dust diffusion and pollution behavior by air curtains based on CFD technology and field measurement. *Build. Environ.* **2019**, *147*, 444–460. [CrossRef]

23. Van Belleghem, M.; Verhaehe, G.; T'Joen, C.; Huisseune, H.; De Jaeger, P.; De Paepe, M. Heat transfer through vertically downward-blowing single-jet air curtains for cold rooms. *Heat Transf. Eng.* **2012**, *33*, 1196–1206. [CrossRef]

24. Goncalves, J.C.; Costa, J.J.; Figueiredo, A.R.; Lopes, A.M.G. Study of the aerodynamic sealing of a cold store—Experimental and numerical approaches. *Energy Build.* **2012**, *55*, 779–789. [CrossRef]

25. Foster, A.M.; Swain, M.J.; Barrett, R.; D'Agaro, P.; James, S.J. Effectiveness and optimum jet velocity for a plane jet air curtain used to restrict cold room infiltration. *Int. J. Refrig.* **2006**, *29*, 692–699. [CrossRef]

26. Moureh, J.; Yataghene, M. Numerical and experimental investigations on jet characteristics and airflow patterns related to an air curtain subjected to external lateral flow. *Int. J. Refrig.* **2016**, *67*, 355–372. [CrossRef]

27. Neto, L.P.C.; Gameiro Silva, M.C.; Cost, J.J. On the use of infrared thermography in studies with air curtain devices. *Energy Build.* **2006**, *38*, 1194–1199. [CrossRef]

28. Hayes, F.C.; Stoecker, W.F. Heat transfer characteristics of the air curtain. *ASHRAE Trans.* **1969**, *1*, 153–167.

29. Gil-Lopez, T.; Castejon-Navas, J.; Galvez-Huerta, M.A.; O'Donohoe, P.G. Energetic, environmental and economic analysis of climatic separation by means of air curtains in cold storage rooms. *Energy Build.* **2014**, *74*, 8–16. [CrossRef]

30. Cordis, Air Curtains on Textile Stenters. Available online: https://cordis.europa.eu/project/rcn/14616/factsheet/en (accessed on 10 January 2018).

31. Sicurfad, Nobilitazione Tessile. Manuale per la Formazione degli Operai. Available online: http://www.sicurfad.it/strumenti/documenti/sicurfadS00.pdf (accessed on 30 November 2018).

32. ANSYS Fluent Theory Guide, ANSYS Inc. Southpointe 2600 ANSYS Drive Canonsburg, PA 15317. January 2019. Available online: http://www.afs.enea.it/project/neptunius/docs/fluent/html/th/node3.htm (accessed on 15 January 2019).

33. Patankar, S.V. *Numerical Heat Transfer and Fluid Flow*; Taylor & Francis: Milton Park, Didcot, UK; Abingdon, UK, 1980; ISBN 978-0-89116-522-4.

34. Montomoli, F.; Massini, M.; Salvadori, S.; Martelli, F. Geometrical Uncertainty and Film Cooling: Fillet Radii. *ASME J. Turbomach.* **2012**, *134*, 011019. [CrossRef]